

See discussions, stats, and author profiles for this publication at: <https://www.researchgate.net/publication/7228086>

# An Interweaving MOF with High Hydrogen Uptake

ARTICLE *in* JOURNAL OF THE AMERICAN CHEMICAL SOCIETY · APRIL 2006

Impact Factor: 12.11 · DOI: 10.1021/ja058777l · Source: PubMed

---

CITATIONS

424

---

READS

43

5 AUTHORS, INCLUDING:



Yanxiong Ke

East China University of Science and Technol...

85 PUBLICATIONS 2,083 CITATIONS

SEE PROFILE



Hong-Cai Zhou

Texas A&M University

234 PUBLICATIONS 19,412 CITATIONS

SEE PROFILE

## An Interweaving MOF with High Hydrogen Uptake

Daofeng Sun, Shengqian Ma, Yanxiong Ke,<sup>†</sup> David J. Collins, and Hong-Cai Zhou\*

Department of Chemistry and Biochemistry, Miami University, Oxford, Ohio 45056

Received December 27, 2005; E-mail: zhouh@muohio.edu

Effective hydrogen storage is needed for fuel-cell vehicles. Single-walled carbon nanotubes, zeolites, activated carbon, and metal hydrides have all been evaluated as possible candidates, but none have met U.S. Department of Energy goals (6.0 wt % for 2010).<sup>1</sup> Recently, metal–organic frameworks (MOFs) have been considered as promising candidates due to exceptionally high porosity, uniform but tunable pore size, and well-defined hydrogen binding sites. MOFs are relatively easy to synthesize with affordable starting materials and straightforward techniques.

Two main strategies can be used to increase the hydrogen uptake of an MOF: increasing the binding energy of H<sub>2</sub> to the network, and increasing the internal surface area and/or pore volume. However, adsorption studies on MOFs, microporous manganese formate, and microporous metal organic materials have shown that there is no direct linear correlation between surface area and hydrogen storage uptake;<sup>2</sup> in fact, many MOFs with high surface area have rather low hydrogen uptake.<sup>3</sup> For this reason, we have focused our studies on increasing the binding energy of hydrogen.

Recently, an inelastic neutron scattering experiment conducted on an MOF (designated MOF-5) developed by Yaghi and co-workers demonstrated two well-defined binding sites: metal-based binding sites and organic linkers.<sup>4</sup> Chen and co-workers have also shown that thermal removal of axial aqua ligands from dicopper paddlewheel secondary building units (SBUs) exposes the copper binding sites in an MOF material.<sup>5</sup>

Several routes to increasing the binding energy of hydrogen to an MOF exist.<sup>6</sup> Smaller pore size increases hydrogen binding, allowing a single H<sub>2</sub> molecule to interact with multiple aromatic rings.<sup>7</sup> Rather than a number of extremely large pores, a larger number of small pores which closely “fit” the dihydrogen molecule is optimal.<sup>8</sup> One route to limiting pore size comes from catenation: interweaving two identical networks with large pores divides the large pores into smaller ones and has the added benefits of increasing both the surface area to pore volume ratio and the overall stability of the network.<sup>7,9</sup> Additionally, the introduction of coordinatively unsaturated metal centers can also increase the hydrogen affinity of the MOF.<sup>5,10</sup>

With these considerations in mind, we have prepared a novel MOF, Cu<sub>3</sub>(TATB)<sub>2</sub>(H<sub>2</sub>O)<sub>3</sub> (TATB = 4,4',4''-s-triazine-2,4,6-triyl-tribenzoate) (**1**). Herein we report the synthesis, structure, and hydrogen adsorption characteristics of **1**.

The three nitrogen atoms in the *s*-triazine ring of the TATB molecule allow the peripheral benzene rings to be coplanar with the central ring (average dihedral angle = 4.5°). This ensures a nearly complete delocalization of  $\pi$  electrons and strong inter-ligand  $\pi$ – $\pi$  interaction, leading to an interweaving MOF. When reacted with copper(II), the carboxylate functionality of TATB leads directly to the formation of the well-understood paddlewheel dicopper SBU, which becomes coordinatively unsaturated upon axial ligand removal.

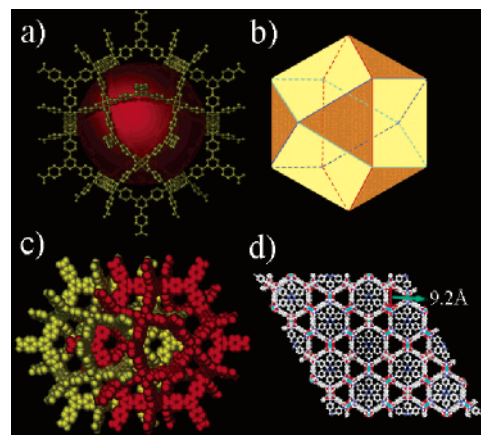


**Figure 1.** (a) A cuboctahedral cage. The red sphere represents the void inside the cage. The distance between opposite corners is 38.0 Å. (b) The four hexagons (red, turquoise, blue, and black) in a cuboctahedron. (c) Two identical interweaving nets represented by two cuboctahedral cages. (d) A view of the packing of **1** from the [001] direction.

Crystals of **1** were formed in the solvothermal reaction of Cu(NO<sub>3</sub>)<sub>2</sub>·2.5H<sub>2</sub>O and H<sub>3</sub>TATB in DMSO at 120 °C. The product was isolated as turquoise crystals of **1**·11H<sub>2</sub>O·3DMSO at 68% yield, with the overall formula determined by crystallography,<sup>11</sup> elemental analysis, and thermogravimetric analysis.

In **1**, dicopper tetracarboxylate paddlewheel SBUs with axial aqua ligands are linked by TATB bridges. Each SBU connects four TATB ligands, and each TATB binds three SBUs to form a *T<sub>d</sub>*-octahedron, which has idealized *T<sub>d</sub>* symmetry with four ligands covering alternating triangular faces of the octahedron and an SBU occupying each vertex. Eight such *T<sub>d</sub>*-octahedra occupy the eight vertices of a cube to form a cuboctahedron through corner sharing, with idealized *O<sub>h</sub>* symmetry (Figure 1a). The average diameter of the void inside the cuboctahedron is 30.3 Å. Every cuboctahedron connects eight *T<sub>d</sub>*-octahedra through face-sharing, and each *T<sub>d</sub>*-octahedron is included in four cuboctahedra, forming a network with *Fm* $\bar{3}$ *m* symmetry.

The overall structure of **1** contains two identical interwoven nets, with the second net generated by a translation of the first by *c*/5 in the [001] direction. The distance of this translation is controlled by the existence of strong  $\pi$ – $\pi$  interactions between two face-to-face stacked TATB ligands; the inter-net distance between the *s*-triazine centers of two ligands is as short as 3.45 Å. Such interaction is typical of *s*-triazine-based systems.<sup>12</sup> This interweaving lowers the overall symmetry of the network from *Fm* $\bar{3}$ *m* to *R* $\bar{3}$ *m*, but does not lower the symmetry of the projection on the (001) plane, which has *p6mm* 2D symmetry, as shown in Figure 1d. The resulting triangular channels are 9.2 Å along an edge, as measured from atom-center to atom-center, and are connected by windows along [110] as small as about 5 Å.

Two similar MOFs constructed with dicopper paddlewheel SBUs exist in the literature: HKUST-1<sup>13</sup> and MOF-14.<sup>14</sup> In HKUST-1,

<sup>†</sup> Current address: Department of Chemical Physics, University of Science and Technology of China, Hefei, China.

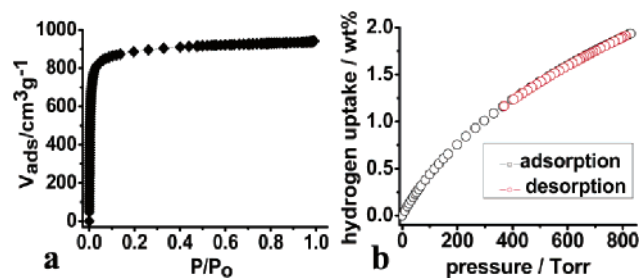


**Figure 2.** Gas sorption isotherms (77 K) of **1** activated at 150 °C: (a) N<sub>2</sub>, (b) H<sub>2</sub>.

the ligand benzene tricarboxylate (BTC) was used as a linker to form a noninterwoven cuboctahedral network. The congruence of the single-net topology can be attributed to ligand shape: like TATB, BTC is nearly planar. However, BTC is much smaller and does not form face-to-face  $\pi$ -stacked pairs—thus explaining the noninterwoven nature of HKUST-1. MOF-14, however, employed the ligand 4,4',4''-benzene-1,3,5-triyltribenzoate (BTB), nearly identical in structure to TATB. However, BTB is nonplanar, with a dihedral angle between central and peripheral rings of 37.1°, due to steric interactions between the hydrogen atoms of the peripheral rings and those of the central ring. This results in a completely different (3,4)-connected Pt<sub>3</sub>O<sub>4</sub>-type topology. Clearly, rational choice of ligand and ligand design can lead to desirable, novel topologies.

Despite the interweaving of the two nets, **1** is still exceptionally porous, with solvent-accessible volume of 74% calculated using PLATON.<sup>15</sup> In the as-isolated form, in addition to the axial aqua ligand on each copper atom, **1** contains 3 DMSO and 11 H<sub>2</sub>O solvates per formula unit. With one of the largest unit cell dimensions ( $c = 80.783$  Å) among all nonprotein structures, crystallographic study can only identify 1 DMSO and 7 H<sub>2</sub>O solvate molecules; the remainder were established by elemental analysis and thermogravimetric analysis.

Compound **1** exhibits permanent porosity, which has been confirmed by gas sorption. Prior to gas sorption experiments, guest solvent molecules and possibly axial aqua ligands are removed by solvent exchange<sup>4b</sup> and thermal activation<sup>5</sup> at an optimized temperature of 150 °C. Activation at higher temperature results in a decrease in measured surface area (see Supporting Information). The N<sub>2</sub> adsorption isotherm, shown in Figure 2a, shows typical Type-I sorption behavior, with a Langmuir surface area of 3800 m<sup>2</sup>/g and a total pore volume of 1.45 mL/g, among the highest surface areas reported in porous materials.<sup>3a,16</sup> The hydrogen adsorption isotherm does not show saturation at 760 Torr (Figure 2b). At 760 Torr and 77 K, **1** adsorbs about 1.9 wt % hydrogen (10.6 mg/cm<sup>3</sup>), which is again among the highest of reported MOF materials.<sup>5,6</sup>

Two reported noninterpenetrating frameworks which have higher surface area are IRMOF-20<sup>6</sup> and MOF-177<sup>3a</sup> (4346 and 4526 m<sup>2</sup>/g, respectively); however, **1** has greater hydrogen adsorption

capacity (1.9 wt % for **1** vs 1.35<sup>6</sup> and 1.25 wt %, <sup>3b</sup> respectively). Hydrogen uptake has also been measured in two additional interpenetrating frameworks, namely, IRMOF-9 and IRMOF-13.<sup>6</sup> However, **1** possesses a higher hydrogen uptake than either (1.17 and 1.73 wt %, respectively).<sup>6</sup> We attribute this to the specific design factors discussed above, namely, the presence of accessible unsaturated metal centers and the existence of pores and channels in a size range well-suited to the dihydrogen molecule. Future work will continue to resolve contributions of these two factors to the hydrogen uptake; investigation is also underway to use TATB and related ligands to create MOFs with higher affinity for hydrogen.

**Acknowledgment.** This work was supported by the National Science Foundation (CHE-0449634), Miami University, and the donors of the American Chemical Society Petroleum Research Fund. H.-C.Z. also acknowledges the Research Corporation for a Research Innovation Award and a Cottrell Scholar Award. The diffractometer was funded by NSF Grant EAR-0003201.

**Supporting Information Available:** Detailed experimental procedures, X-ray structural determination, powder diffraction patterns, and thermogravimetric analysis. This material is available free of charge via the Internet at <http://pubs.acs.org>.

## References

- (1) Hydrogen, Fuel Cells & Infrastructure Technologies Program: Multi-year Research, Development, and Demonstration Plan. U.S. Department of Energy, 2005, <http://www.eere.energy.gov/hydrogenandfuelcells/mypp/>.
- (2) Pan, L.; Sander, M. B.; Huang, X.; Li, J.; Smith, M. R., Jr.; Bittner, E. W.; Bockrath, B. C.; Johnson, J. K. *J. Am. Chem. Soc.* **2004**, *126*, 1308.
- (3) (a) Chae, H. K.; Siberio-Pérez, D. Y.; Kim, J.; Go, Y. B.; Eddaoudi, M.; Matzger, A. J.; O'Keeffe, M.; Yaghi, O. M. *Nature* **2004**, *427*, 523. (b) Rowsell, J. C.; Millward, A. R.; Park, K. S.; Yaghi, O. M. *J. Am. Chem. Soc.* **2004**, *126*, 5666.
- (4) (a) Rosi, N. L.; Eckert, J.; Eddaoudi, M.; Vodak, D. T.; Kim, J.; O'Keeffe, M.; Yaghi, O. M. *Science* **2003**, *300*, 1127. (b) Rowsell, J. L. C.; Eckert, J.; Yaghi, O. M. *J. Am. Chem. Soc.* **2005**, *127*, 14904.
- (5) Chen, B. L.; Ockwig, N. W.; Millward, A. R.; Contreras, D. S.; Yaghi, O. M. *Angew. Chem., Int. Ed.* **2005**, *44*, 4745.
- (6) Rowsell, J. L. C.; Yaghi, O. M. *J. Am. Chem. Soc.* **2006**, *128*, 1304.
- (7) Kesani, B.; Cui, Y.; Smith, M. R., Jr.; Bittner, E. W.; Bockrath, B. C.; Lin, W. *Angew. Chem., Int. Ed.* **2005**, *44*, 72.
- (8) Chun, H.; Dybtsev, D. N.; Kim, H.; Kim, K. *Chem.—Eur. J.* **2005**, *11*, 3521.
- (9) Rowsell, J. L. C.; Yaghi, O. M. *Angew. Chem., Int. Ed.* **2005**, *44*, 4670.
- (10) (a) Kaye, S. S.; Long, J. R. *J. Am. Chem. Soc.* **2005**, *127*, 6505. (b) Dinca, M.; Long, J. R. *J. Am. Chem. Soc.* **2005**, *127*, 9376.
- (11) Crystal data for **1**: Cu<sub>3</sub>C<sub>48</sub>H<sub>30</sub>N<sub>6</sub>O<sub>15</sub>,  $M = 1121.4$ , rhombohedral, space group  $R\bar{3}m$ ,  $T = 293(2)$  K,  $a = 32.9680(13)$ ,  $c = 80.783(5)$  Å,  $V = 76039(6)$  Å<sup>3</sup>,  $Z = 24$ ,  $\rho_{\text{calc}} = 0.588$  g/cm<sup>3</sup>,  $R_1 = 0.053$ ,  $wR_2 = 0.15$ .
- (12) (a) Ke, Y.; Collins, D. J.; Sun, D.; Zhou, H.-C. *Inorg. Chem.* **2006**, *45*, 1897. (b) Jessiman, A. S.; MacNicol, D. D.; Mallinson, P. R.; Vallance, I. J. *Chem. Soc., Chem. Commun.* **1990**, 1619. (c) Sponer, J.; Hobza, P. *Chem. Phys. Lett.* **1997**, *267*, 263. (d) Thalladi, V. R.; Boese, R.; Brasselet, S.; Ledoux, I.; Zyss, J.; Jetli, R. K. R.; Desiraju, G. R. *Chem. Commun.* **1999**, 1639. (e) Sun, D.; Ma, S.; Ke, Y.; Petersen, T. M.; Zhou, H.-C. *Chem. Commun.* **2005**, 2663.
- (13) Chui, S. S.-Y.; Lo, S. M.-F.; Charmant, J. P. H.; Orpen, A. G.; Williams, I. D. *Science* **1999**, *283*, 1148.
- (14) Chen, B.; Eddaoudi, M.; Hyde, S. T.; O'Keeffe, M.; Yaghi, O. M. *Science* **2001**, *291*, 1021.
- (15) Spek, A. L. *J. Appl. Crystallogr.* **2003**, *36*, 7.
- (16) Férey, G.; Mellot-Draznieks, C.; Serre, C.; Millange, F.; Dutour, J.; Surlle, S.; Margiolaki, I. *Science* **2005**, *309*, 2040.

JA058777L